

# Full-length Dysferlin Transfer by the Hyperactive *Sleeping Beauty* Transposase Restores Dysferlin-deficient Muscle

Helena Escobar<sup>1</sup>, Verena Schöwel<sup>2</sup>, Simone Spuler<sup>2</sup>, Andreas Marg<sup>2</sup> and Zsuzsanna Izsvák<sup>1</sup>

Dysferlin-deficient muscular dystrophy is a progressive disease characterized by muscle weakness and wasting for which there is no treatment. It is caused by mutations in *DYSF*, a large, multiexonic gene that forms a coding sequence of 6.2 kb. *Sleeping Beauty* (SB) transposon is a nonviral gene transfer vector, already used in clinical trials. The hyperactive SB system consists of a transposon DNA sequence and a transposase protein, SB100X, that can integrate DNA over 10 kb into the target genome. We constructed an SB transposon-based vector to deliver full-length human *DYSF* cDNA into dysferlin-deficient H2K A/J myoblasts. We demonstrate proper dysferlin expression as well as highly efficient engraftment (>1,100 donor-derived fibers) of the engineered myoblasts in the skeletal muscle of dysferlin- and immunodeficient B6.Cg-*Dysf*<sup>prmd</sup> *Prkdc*<sup>scid</sup>/J (Scid/BLA/J) mice. Nonviral gene delivery of full-length human dysferlin into muscle cells, along with a successful and efficient transplantation into skeletal muscle are important advances towards successful gene therapy of dysferlin-deficient muscular dystrophy.

*Molecular Therapy—Nucleic Acids* (2016) 5, e277; doi:10.1038/mtna.2015.52; published online 19 January 2016

**Subject Category:** Gene insertion deletion or modification

## Introduction

Miyoshi myopathy, limb girdle muscular dystrophy 2B, and distal anterior compartment myopathy are autosomal recessive muscle disorders caused by mutations in the gene encoding dysferlin (*DYSF*).<sup>1–3</sup> They are encompassed by the term dysferlinopathy and affect the proximal and/or distal muscles of the limbs. They generally appear after puberty and their clinical presentation is variable regarding the types of muscles involved and the degree of severity.<sup>1–3</sup> Patients usually become wheelchair-bound within 10–20 years of disease onset due to progressive muscle degeneration, weakness, and atrophy.

*DYSF* spans over 150 kb of genomic DNA in chromosome 2p13 and comprises 55 exons that form a coding sequence of 6.2 kb.<sup>1,2,4</sup> The 237 kDa dysferlin protein belongs to the ferlin family, a group of large proteins with important roles in vesicle trafficking and fusion.<sup>5</sup> *DYSF* is expressed in several tissues, including kidney and immune cells, but its highest expression was reported in muscle,<sup>6</sup> where dysferlin is mainly detected in mature myofibers.<sup>7</sup> In muscle fibers, dysferlin localizes predominantly to the sarcolemma, but it is also present at the transverse tubules.<sup>6,8,9</sup> Dysferlin has a well-studied role in membrane repair, an important process in muscle fibers, which are continually subject to mechanical stress-induced injuries. Mutations in *DYSF* have been exclusively associated with skeletal muscle diseases. Absence of dysferlin leads to impaired resealing of sarcolemmal wounds.<sup>10</sup> Defects in dysferlin are also known to cause increased inflammatory attack to muscle fibers, which contributes to the exacerbation of the muscle pathology.<sup>11,12</sup>

Currently, there is no treatment for dysferlinopathy. Given that a single gene is causative for the pathology, gene therapy holds great promise. However, the large size of the *DYSF* coding sequence represents a challenge for gene transfer approaches, since most viral vectors used in gene therapy have a lower cargo capacity. *Sleeping Beauty* (SB) transposon is a nonviral genetic tool widely used for stable gene transfer in various cell types.<sup>13</sup> This plasmid-based, bi-component system consists of a transposon DNA sequence and a transposase protein that excises the transposon from the donor plasmid and integrates it into the target genome. The transposon can be engineered to carry any gene of interest. Although the efficacy of transposase-mediated transgene insertion decreases with increasing cargo size,<sup>14,15</sup> the hyperactive SB100X transposase is still capable of integrating large, over 10 kb or even BAC-size DNA.<sup>16</sup> Thus, the SB system is well suited to deliver large sequences, such as the *DYSF* coding sequence. Most importantly, the SB system has already been used in a clinical setup.<sup>17</sup> We constructed an SB transposon-based vector to deliver the full-length human *DYSF* cDNA into dysferlin-deficient H2K myoblasts (H2K A/J).<sup>18</sup> H2K myoblasts are conditionally immortalized through expression of the tsA58 thermosensitive SV40 large-T-antigen driven by the *H-2K<sup>b</sup>* promoter.<sup>19</sup> They have extensive proliferative capacity *in vitro* and can engraft robustly into muscle, offering a proper model to test the feasibility of our therapeutic strategy consisting of stably expressing full-length *DYSF* using the SB system.<sup>19</sup> H2K A/J myoblasts are derived from dysferlin-null mice, harboring a homozygous *Dysf*<sup>prmd</sup> mutation<sup>20</sup> and the *H-2K<sup>b</sup>*tsA58 allele.<sup>21</sup> Our strategy involved the optimization of a pretransplantation treatment

The last two authors contributed equally to this work.

<sup>1</sup>Mobile DNA, Max Delbrück Center for Molecular Medicine of the Helmholtz Society, Berlin, Germany; <sup>2</sup>Muscle Research Unit, Experimental and Clinical Research Center (ECRC), a joint cooperation between the Charité, Universitätsmedizin Berlin and the Max Delbrück Center for Molecular Medicine, Berlin, Germany. Correspondence: Zsuzsanna Izsvák, Max Delbrück Center for Molecular Medicine, Robert-Rössle Str. 10, 13125 Berlin, Germany. E-mail: zizsvak@mdc-berlin.de or Andreas Marg, Muscle Research Unit, ECRC, Lindenberger Weg 80, 13125 Berlin, Germany. E-mail: andreas.marg@charite.de

**Keywords:** dysferlin; gene therapy; myoblast transplantation; *Sleeping Beauty* transposon

Received 13 November 2015; accepted 13 November 2015; advance online publication 19 January 2016. doi:10.1038/mtna.2015.52

by combining irradiation and cardiotoxin (CTX) injection. Our results demonstrate proper dysferlin reconstitution as well as highly efficient engraftment of engineered myoblasts in dysferlin- and immunodeficient B6.Cg-*Dysf<sup>prmd</sup>* *Prkdc<sup>scid</sup>*/J (Scid/BLA/J) mice.<sup>22</sup>

## Results

### H2K A/J muscle cells properly express full-length human DYSF following SB-mediated gene transfer

To ensure optimal expression of the therapeutic gene, we chose the synthetic c5-12 (Spc5-12) promoter.<sup>23</sup> The Spc5-12 promoter was constructed by random assembly of evolutionarily conserved transcription factor binding sites, providing tissue specificity in adult skeletal muscle. Importantly, the Spc5-12 promoter was shown to drive strong transgene expression *in vitro* in myoblasts and myotubes<sup>23</sup> and *in vivo* in mouse myofibers.<sup>24,25</sup> The size of the Spc5-12 promoter is <400 bp. In our hands, a duplicate of Spc5-12 (2xSpc5-12) regulatory sequence proved to be the most efficient in driving transgene expression in H2K A/J myoblasts. We generated a bicistronic vector, in which the full-length human *DYSF* cDNA was followed by a GFP reporter. GFP was preceded by an Internal Ribosome Entry Site (IRES) sequence to allow simultaneous translation of both cistrons (pT2-2xSpc5-12-hDYSF-IRES-GFP; short: hDYSF-IRES-GFP) (Figure 1a).  $2 \times 10^6$  H2K A/J myoblasts were electroporated with 2  $\mu$ g of hDYSF-IRES-GFP and 200 ng of an expression vector for SB100X transposase.<sup>15</sup> The engineered cells were selected by FACS sorting for the GFP signal after 11 days. At this time, the background GFP<sup>+</sup> signal deriving from nonintegrated plasmid DNA could no longer be detected (Supplementary Figure S1). Due to the rather low transfection rate of the large therapeutic plasmid (2–3%), we enriched the culture for GFP<sup>+</sup> cells through three rounds of cell sorting to obtain a population of 98.6% positive cells (Figure 1b).

Next, we analyzed FACS-sorted, GFP<sup>+</sup> H2K A/J myoblasts and differentiated myotubes for dysferlin expression by western blot and immunohistochemistry (Figure 1c,d). Dysferlin was detected in low amounts in engineered H2K A/J myoblasts, but its expression level increased with differentiation (Figure 1c). H2K A/J cells not engineered or engineered with an SB-based vector encoding only a GFP reporter (pT2-CAG-IRES-GFP) did not express dysferlin (Figure 1c). Dysferlin-immunofluorescence revealed strong membrane staining in engineered myotubes (Figure 1d). These experiments indicate that dysferlin expression in corrected H2K A/J cells (H2K A/J-DYSF<sup>+</sup>) follows the physiological time and spatial distribution.

### Corrected H2K A/J myoblasts can efficiently be transplanted into Scid/BLA/J mouse muscle

We next asked whether corrected and FACS-sorted H2K A/J myoblasts would be capable of reconstituting dysferlin *in vivo* following transplantation into the *tibialis anterior* (TA) muscle of Scid/BLA/J mice. The abrogation of the regenerative capacity of the host muscle by irradiation has been shown to enhance the engraftment of donor cells.<sup>26</sup> We used a recently developed method for highly precise focal irradiation of mouse hind limbs using an image guided radiosurgery

robot<sup>27</sup> and transplanted  $3 \times 10^5$  H2K A/J-DYSF<sup>+</sup> myoblasts into 18 Gy irradiated TA muscles of Scid/BLA/J mice.<sup>22</sup> Using immunohistochemistry, we detected up to 140 dysferlin-positive fibers in muscles collected 3 ( $n = 2$ ) and 6 weeks ( $n = 2$ ) posttransplantation (Figure 2a,b, left columns). These data suggest that the donor myoblasts engrafted successfully and gave rise to dysferlin expressing myofibers in the host muscle. Next, we stimulated regeneration in the host muscles using CTX, a strategy reported to improve engraftment of donor myoblasts.<sup>28</sup> CTX causes myofiber degeneration and necrosis, resulting in acute damage-induced muscle regeneration, but it does not damage satellite cells.<sup>26,29</sup> In order to induce a regenerative environment, we treated the TA muscles of Scid/BLA/J mice with CTX at the same time point at which  $3 \times 10^5$  H2K A/J-DYSF<sup>+</sup> myoblasts were injected. This injury model resulted in a dramatic increase in dysferlin-positive fibers in the transplanted TA muscles (Figure 2a,b, middle and right columns). We counted 500–1,100 dysferlin-positive muscle fibers/cross-sectional area, extending a length of at least 5 mm, 3 weeks posttransplantation ( $n = 2$ ) (Figure 2a, middle and right columns). We still detected 400–1,000 dysferlin expressing fibers/cross sectional area in muscles collected 6 weeks posttransplantation ( $n = 2$ ) (Figure 2b, middle and right columns). Per section, the area of the transplant extended up to  $1,000 \times 800 \mu\text{m}$ . As in healthy muscle, dysferlin was mainly expressed at the sarcolemma. No dysferlin-positive fibers were detected in the control muscles that were only irradiated or injected with CTX (not shown).

### Muscle regeneration using H2K A/J-DYSF<sup>+</sup> cells appears morphologically normal

We next investigated whether transplants derived from H2K A/J-DYSF<sup>+</sup> myoblasts would properly regenerate muscle. Serial cryosections from transplanted TA muscles were immunostained for dysferlin to identify the transplanted area. H&E (Hematoxylin and Eosin), Gomori Trichrome, and NADH-dehydrogenase stains revealed that the grafted area was sharply demarcated towards the host muscle. There was only a mild increase in connective tissue mass between host- and graft-derived muscle. Grafted muscle displayed all typical features of regeneration, including large variation of fiber size, internalized nuclei in a high percentage of fibers, loose tissue structure, and lack of inflammatory infiltrates (Figure 3).

### H2K A/J-DYSF<sup>+</sup> muscle cells gave rise to multiple Pax7-positive cells

Myonuclei of mature fibers are postmitotic and the *de novo* nuclei are provided exclusively by myoblast–myoblast or myoblast-to-myofiber fusion. Therefore, only engraftment of a subset of donor-derived cells as satellite cells would ensure contribution to muscle regeneration in pathological circumstances and a long-lasting therapeutic effect.<sup>28</sup> Satellite cells can be identified by their expression of the transcription factor Pax7<sup>30</sup> and their localization beneath the basal lamina of myofibers.<sup>31</sup> We found cells positive for the expression of both Pax7 and dysferlin. A few of them located underneath forming basal lamina structures identified by laminin staining, but many of them had not yet adopted a satellite cell position and were interstitial (Figure 4).

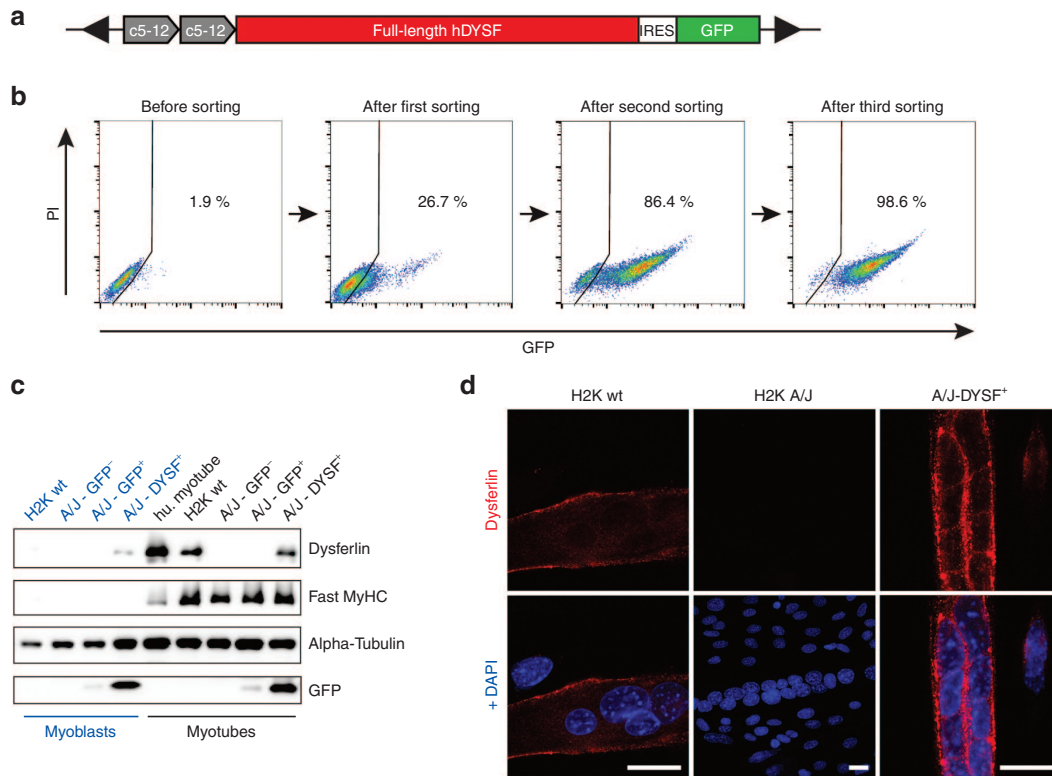


**Figure 1 Restoration of full-length dysferlin expression in H2K A/J muscle cells.** (a) Schematic view of the *Sleeping Beauty* (SB)-based full-length, human dysferlin transfer vector (hDYSF-IRES-GFP). Black arrows: transposon inverted terminal repeats. (b) Enrichment of the H2K A/J - *DYSF*<sup>+</sup> population. hDYSF-IRES-GFP plus an expression vector for SB100X transposase were transfected into H2K A/J myoblasts and enriched by three rounds of FACS sorting, resulting in a 98.6% GFP<sup>+</sup> cell population. (c) Immunoblot demonstrating dysferlin reconstitution in H2K A/J myoblasts (blue) and myotubes (black) (A/J-*DYSF*<sup>+</sup>GFP<sup>+</sup>). Note that dysferlin is expressed at a higher level in myotubes than in myoblasts. No dysferlin is detected in H2K A/J cells that had not received the hDYSF-IRES-GFP-vector. Additional controls were myoblasts and myotubes stably transfected with an SB-based vector encoding only a GFP reporter driven by the ubiquitous CAG promoter (pT2-CAG-IRES-GFP) and sorted for selecting the GFP-positive (A/J-GFP<sup>+</sup>) and negative (A/J-GFP<sup>-</sup>) populations. Hu.myotubes, normal primary human myotubes. Fast MyHC, fast myosin heavy chain. (d) Immunostaining of dysferlin (red; Romeo ab) in H2K wt, H2K A/J, and H2K A/J-*DYSF*<sup>+</sup> myotubes. Sarcolemmal dysferlin staining is shown in dysferlin-negative H2K A/J cells reconstituted with hDYSF-IRES-GFP. Blue, DAPI. Bars = 20 μm. DAPI, 4',6-diamidino-2-phenylindole; IRES, Internal Ribosome Entry Site; PI, propidium iodide.

## Discussion

Here, we describe a proof of principle of an SB-based gene transfer into mouse myoblasts. In the last decades, several approaches have been taken to restore dysferlin function in dysferlinopathies. In allogeneic cell transplantation studies, dysferlin expression was reconstituted in mouse myofibers by transplanting labeled wild-type mouse myoblasts into SJL mice.<sup>32</sup> In addition, expression of human dysferlin could be detected following intramuscular transplantation of human control myoblasts into SCID mice.<sup>32</sup> In gene therapy studies, adeno-associated viral (AAV) vectors have been extensively investigated for dysferlin gene transfer. Due to their limited cargo capacity, AAV vectors cannot deliver the full-length *DYSF* coding sequence. However, in very elegant approaches using the high intermolecular recombination ability of AAVs, it was possible to transfer the 5' and 3' moiety of the *DYSF* cDNA in two separate vectors, achieving robust full-length dysferlin protein reconstitution *in vivo*.<sup>33–35</sup> Dual AAV-mediated dysferlin expression has been shown to persist for >1 year in mouse skeletal muscle.<sup>35</sup> However, AAV vectors are non-self-replicating

and long-term treatment of patients with skeletal muscle disorders may require repeated vector administrations, with the possible complication of immune responses against the viral capsid.<sup>36</sup>

The use of lentiviral vectors has enabled the successful delivery of full-length dysferlin into patient-derived CD133<sup>+</sup> cells *in vitro*, but the results *in vivo* have so far been discouraging.<sup>37</sup> In addition, there have been attempts to use RNA-based strategies like exon skipping or *trans*-splicing to treat dysferlinopathies. Exon 32 of *DYSF* might be dispensable for protein function, since a patient harboring a mutation in this exon developed a mild disease phenotype.<sup>38</sup> Successful targeting of exon 32 to induce exon skipping has been shown *in vitro* using antisense oligonucleotides.<sup>39</sup> Furthermore, our laboratory demonstrated successful spliceosome-mediated *trans*-splicing of the *DYSF* pre-mRNA both *in vitro* and *in vivo*.<sup>40</sup> Despite of the encouraging *in vitro* results, *in vivo* dysferlin protein restoration using RNA-based therapies has remained very limited.<sup>39–41</sup> Our current work using *ex vivo* delivery of an SB transposon-based therapeutic construct has provided the most efficient results so far, in terms of engraftment and dysferlin protein restoration of any cell



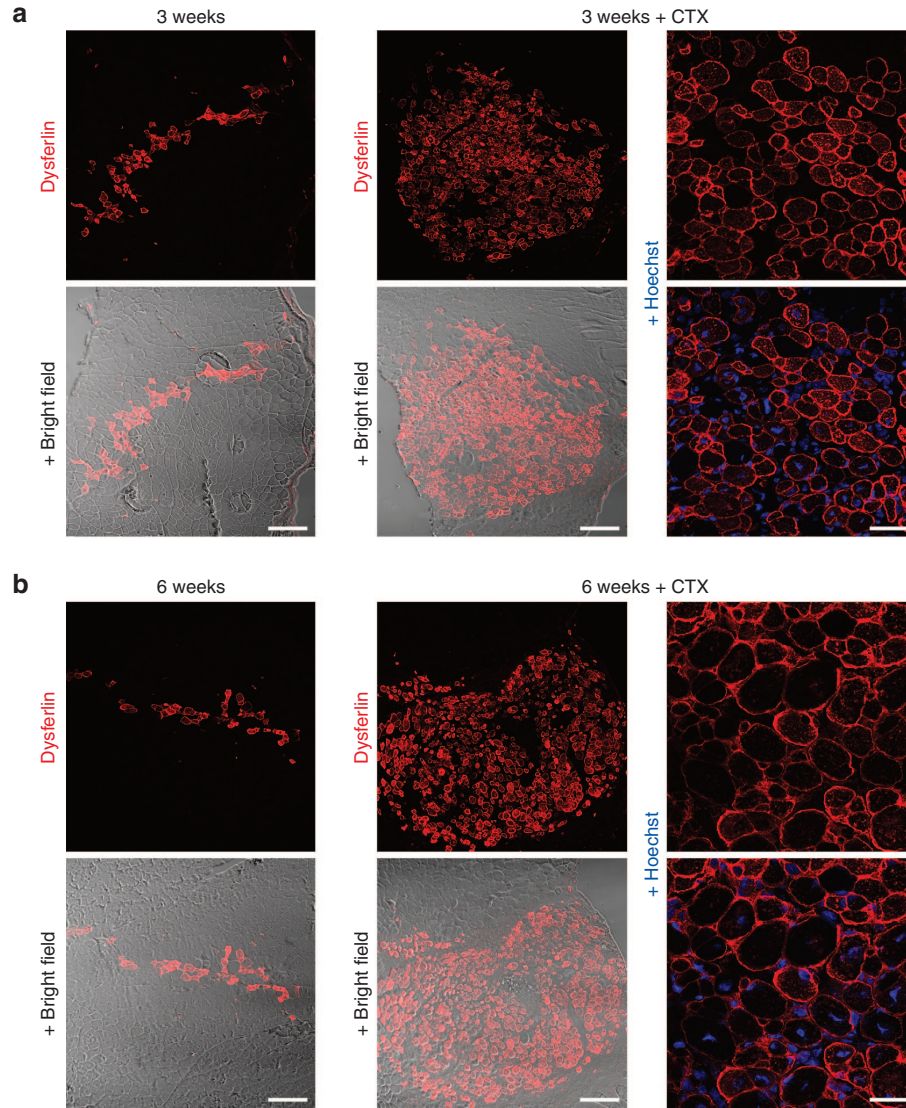


**Figure 2 Robust dysferlin reconstitution in skeletal muscle of Scid/BLA/J mice following transplantation of engineered myoblasts.**

About  $3 \times 10^5$  H2K A/J-DYSF<sup>+</sup> myoblasts were transplanted into the tibialis anterior (TA) muscles of Scid/BLA/J mice 1 day after local 18 Gy irradiation. Representative images of cryosections from TA muscles collected 3 weeks (a) or 6 weeks (b) after transplantation and immunostained with an anti-dysferlin ab (red; Romeo ab). Blue, Hoechst. While donor-derived myofibers expressing dysferlin were present at low numbers (up to 140 fibers) in muscles that were only irradiated (a,b – left columns), they were very abundant (~500 to 1,100 after 3 weeks and ~400 (note that this number may be underestimated) to 1,000 after 6 weeks) and occupied large areas of grafted muscles (max. area of  $1,000 \times 800 \mu\text{m}$ ) that were subjected to a combined pretreatment of irradiation and CTX injection (a,b – middle and right columns). Dysferlin was enriched at the membrane of the donor-derived myofibers (a,b – right columns). CTX, cardiotoxin. Bars = 200  $\mu\text{m}$  (left and middle columns)/50  $\mu\text{m}$  (right columns).

therapy or cell-based gene therapy studies in dysferlin-deficient mouse models.

We have transplanted engineered H2K A/J myoblasts into the TA muscles of Scid/BLA/J mice. We determined engraftment efficiency based on the presence of donor-derived myofibers, expressing dysferlin. We could use dysferlin expression directly to monitor engraftment, as mice carrying a homozygous *Dysf<sup>pmid</sup>* allele do not express any dysferlin protein.<sup>20,22</sup> Accordingly, we did not detect any dysferlin-positive fibers in nongrafted muscles of Scid/BLA/J mice that were uninjured, irradiated only, or had just received CTX.

Immortalized C2C12 mouse myoblasts have been shown to rapidly form tumors when transplanted into TA muscles of *mdx nu/nu* and nondystrophic *beige/nu/Xid* mice.<sup>42</sup> In those studies, tumor formation was especially evident in muscles that had been irradiated. H2K myoblasts are only conditionally immortalized and are not expected to form tumors *in vivo*. Still, spontaneous transformation during *in vitro* culturing could occur and might result in tumor formation following grafting into an immunosuppressed model. Notably, we did not observe any tumors in the grafted muscles or the surrounding tissues at any of the examined time points,

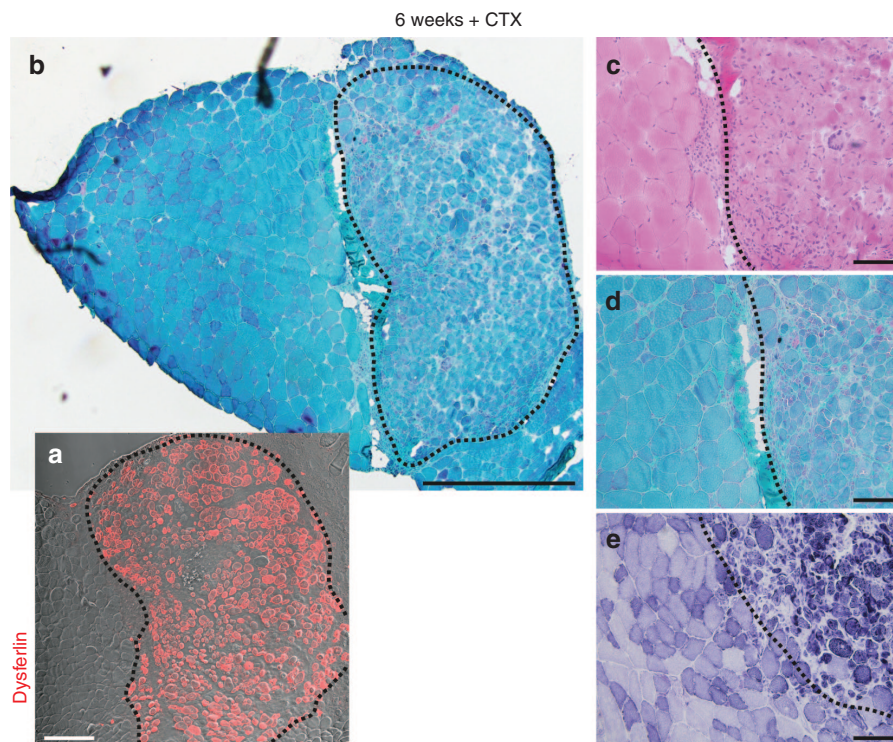


**Figure 3 Donor-derived muscle shows histological features of regeneration.** Images of histological stains on cryosections from a grafted muscle collected 6 weeks after cell transplantation and injection of CTX. (a) The area containing donor-derived myofibers is indicated in a cryosection from the same muscle immunostained with an anti-dysferlin ab (red; Romeo ab). Bar = 200  $\mu\text{m}$ . (b) The delineation of the same area in a low magnification image of a Gomori Trichrome stain shows its large size and its clear demarcation from areas containing only host myofibers. Bar = 500  $\mu\text{m}$ . (c–e) Donor-derived muscle shows hallmarks of regeneration, including higher fiber size variation, rounded myofibers, edematous interstitial space, basophilic fibers, and central nuclei as evidenced by the Hematoxylin and Eosin (c), NADH-dehydrogenase (d), and Gomori Trichrome (e) stains. Bars = 100  $\mu\text{m}$ . CTX, cardiotoxin.

suggesting that the transplanted pool was free of cells spontaneously transformed in culture.

In our hands, a pretransplantation treatment consisting of a combination of irradiation with CTX injection improved engraftment as compared to irradiation alone. Although it is accepted that inactivation of the endogenous satellite cells by radiation or cryoinjury is beneficial for the engraftment of donor cells, the role of additional injury using myotoxins is rather controversial.<sup>26,43</sup> The differences in transplantation efficacy might be partially explained by technical reasons. Also, each disease and engraftment model may require a specific pretransplantation treatment that needs to be optimized individually. In this regard, it is important to note that muscle regeneration only occurs when Pax7-positive satellite cells, the proper stem cells of skeletal muscle, are present in the tissue.<sup>44,45</sup> In agreement with this assumption, engraftment and contribution to myofibers of nonmuscle stem cell types, like mesoangioblasts or CD133<sup>+</sup> cells, have only been demonstrated in nonirradiated muscles of Scid/BLA/J mice, injured with myotoxins only, where the endogenous satellite cells were intact.<sup>37,46</sup> Our results clearly support the positive role of a double injury model. Although formation of functional satellite cells by transplanted myoblasts has been reported,<sup>19,47</sup> the detection of multiple Pax7-positive, dysferlin-positive cells in the graft's area was unexpected because engineered H2K A/J myoblasts had been extensively expanded *ex vivo* prior to transplantation. Whether donor-derived satellite cells

with true stem cell characteristics were established remains unresolved.

Our SB-based approach can theoretically be applied to all loss-of-function mutations in *DYSF*. The effect of SB-mediated *DYSF* delivery is more difficult to foresee in dysferlinopathies caused by missense mutations in *DYSF*. In these individuals, the residual dysferlin protein might be accumulated, resulting in aggregates within the muscle cell.<sup>48</sup> In these cases, the suitability of this therapeutic approach must first be assessed *in vitro*, since overexpression of dysferlin might cause a myopathy itself.<sup>49</sup> In principle, SB could be used to deliver genes relevant for other muscular dystrophies as well. SB has several advantageous features compared with other integrating vectors, including a potentially safer, close-to-random genomic integration profile versus lentivirus or other transposon-based systems.<sup>50,51</sup> Furthermore, since it is a plasmid-based system, it is simple and inexpensive to manufacture, which represents a substantial benefit for clinical use. Maintenance of human primary myoblast cultures, however, is labor intensive and expensive. On the other hand, it remains to be established how human muscle needs to be prepared in order to accept autologous myoblast transplants. If needed, more gentle or alternative treatments to render patients' muscles receptive to grafts, while avoiding irreversible tissue damage, should be evaluated.

Altogether, our results show nonviral integration of full-length human dysferlin into muscle cells as well as successful, efficient transplantation into skeletal muscle. These



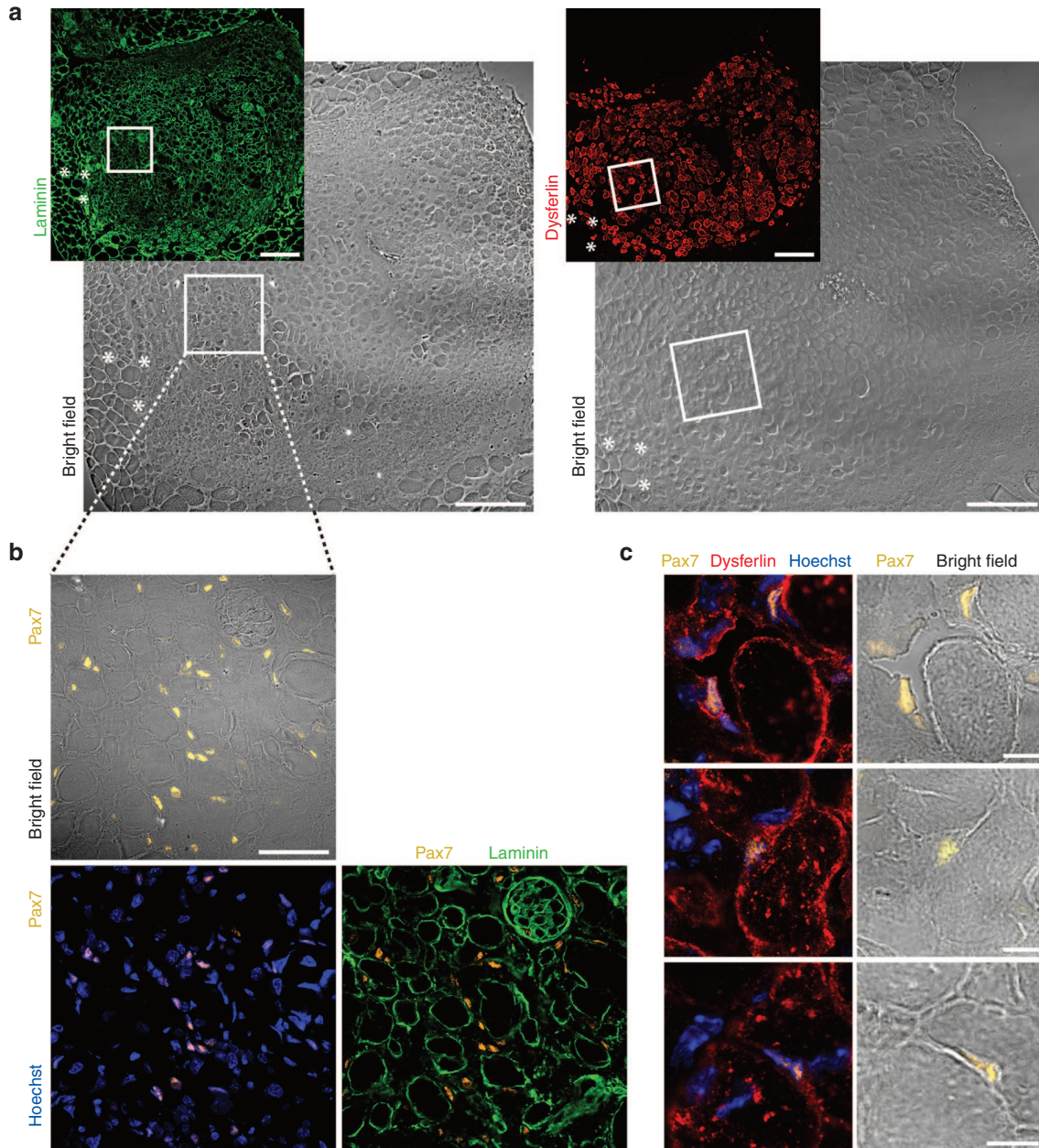


**Figure 4 Engineered myoblasts of donor origin gave rise to numerous Pax7<sup>+</sup> cells in grafted muscles.** (a) Corresponding areas stained for dysferlin (red) and for laminin (green) in serial sections from a grafted muscle 6 weeks after transplantation of H2K A/J-DYSF<sup>+</sup> myoblasts. The asterisks (\*) and squares indicate the same areas in the left and right images. The squares indicate the area shown in **b**. Bars = 200  $\mu$ m. (b) Numerous Pax7<sup>+</sup> (ochre) cells are present in areas containing donor-derived myofibers. Some cells are located beneath forming basal lamina (green) structures and most of them are interstitial. Blue, Hoechst. Bar = 50  $\mu$ m. (c) Pax7<sup>+</sup> cells (ochre) coexpress dysferlin (red; Romeo ab) and are located next to donor-derived myofibers. Blue, Hoechst. Bars = 10  $\mu$ m.

are important advances towards successful autologous cell-based gene therapy of dysferlin-deficient muscular dystrophy. Further efforts are needed to enable translation of our findings into clinical use in patients.

#### Materials and methods

**Plasmid vectors.** The SB100X expression vector was previously described.<sup>15</sup> The SB-based reporter vector pT2-CAG-IRES-GFP was kindly provided by Angélica García Pérez,

Max Delbrück Center for Molecular Medicine, Berlin. The SB-based vector for full-length dysferlin transfer (hDYSF-IRES-GFP) was constructed as follows: the full-length human dysferlin coding sequence (accession #DQ267935) was extracted from the pDONR221:15803 plasmid (provided by The Jain Foundation) with *SpeI* + *NotI* and cloned into an empty SB transposon plasmid<sup>52</sup> previously digested with *XbaI* + *NotI* (resulting vector - pT2-hDYSF). The *Spc5-12* promoter sequence was extracted from pAAV-Spc5-12-huDysco (Kindly provided by George Dickson, Royal Holloway

University of London) with XbaI. Two copies of the Spc5-12 sequence were inserted in tandem in a 5' to 3' orientation into pT2-hDYSF digested with SpeI (resulting vector - pT2-2xSpc5-12-hDYSF). The IRES-GFP-poly(A) sequence was PCR-amplified from pT2-CAG-IRES-GFP with Pfu Ultra II Fusion DNA polymerase (Agilent Technologies, Santa Clara, CA) using the forward 5'-ATCTGCGGCCGCTAGCCAATTCCGCCCTC-3' and reverse 5'-TCTTGC GGCCGCTGTACAACTAGTCGATCCCTCTTAAGTACCAC-3' primers. The resulting PCR fragment was digested with NotI and inserted into pT2-2xSpc5-12-hDYSF previously digested with NotI.

**Cell culture.** Conditionally immortalized H2K and H2K A/J myoblasts<sup>18</sup> were a gift from Terence Partridge, National Children's Hospital, Bethesda, MD. Cells were cultured on dishes coated with 0.1% gelatin from porcine skin (Sigma-Aldrich, Saint Louis, MO). H2K myoblasts were routinely tested for mycoplasma and experiments were only performed using mycoplasma-free cells. To allow proliferation, H2K myoblasts were cultured at 33 °C and 10% CO<sub>2</sub> in Dulbecco's Modified Eagle Medium high glucose supplemented with GlutaMAX and pyruvate (Gibco, Life Technologies, Carlsbad, CA), 1× Antibiotic-Antimycotic (Gibco, Life Technologies), 20% fetal calf serum (PAA Laboratories, Pasching, Austria), 2% chick embryo extract (US Biological, Salem, MA), and 200 U/ml of  $\gamma$ -interferon (Merck Millipore, Darmstadt, Germany). For differentiation, cells were placed into 37 °C and 5% CO<sub>2</sub> for 7 days in proliferation media devoid of  $\gamma$ -interferon and subsequently switched into Dulbecco's Modified Eagle Medium containing Antibiotic-Antimycotic, 5% horse serum (Gibco, Life Technologies), and 2% chick embryo extract. Primary human myoblasts were isolated and purified as previously described.<sup>53</sup> In brief, cells were grown in Skeletal Muscle Growth Medium (PromoCell, Heidelberg, Germany) supplemented with 10% fetal calf serum (Lonza, Basel, Switzerland), 2.72 mmol/l GlutaMAX, and 400  $\mu$ g/ml gentamicin (Gibco, Life Technologies). Differentiation into myotubes was induced in Dulbecco's Modified Eagle Medium containing 2% horse serum (Gibco, Life Technologies).

**Transfection and sorting of H2K A/J myoblasts.** H2K A/J myoblasts were transfected with a Neon Transfection System (Life Technologies). An electroporation protocol consisting of 1,050 mV, 30 ms, 2 pulses was selected due to an optimal ratio between transfection efficiency and cell viability. Thoroughly washed cells were aliquoted according to the number of cells needed for each transfection. Each aliquot was resuspended in buffer R (Neon Transfection System, Life Technologies) containing plasmid DNA and electroporated according to the manufacturer's instructions. Immediately after electroporation, cells were plated in gelatin-coated dishes containing H2K myoblast proliferation media. Routine flow cytometry to monitor expression of GFP was performed using a FACSCalibur flow cytometer (BD Biosciences, Franklin Lakes, NJ) and analysis of the flow cytometry data was performed with the Cellquest Pro (BD Biosciences) and FlowJo Softwares. Sorting of GFP expressing H2K A/J myoblasts was done using a FACSaria flow cytometer (BD Biosciences).

**Sodium dodecyl sulfate–polyacrylamide gel electrophoresis and immunoblot.** For immunoblotting, myoblasts or myotubes were lysed on ice with radioimmunoprecipitation assay buffer (50 mmol/l Tris–HCl, 150 mmol/l NaCl, 0.1% NP-40, 0.1% sodium dodecyl sulfate, 0.1% sodium deoxycholate, and protease inhibitors). The protein concentration was determined using BCA Protein Assay Kit (Thermo Fisher Scientific, Waltham, MA). For each sample, 10  $\mu$ g protein diluted in sample buffer (0.25 mol/l Tris–HCl, 50% glycerol, 5% sodium dodecyl sulfate, 0.05% bromophenol blue, and 10% freshly added  $\beta$ -mercaptoethanol) were loaded onto a Novex 8–16% gradient Tris–glycine Mini Protein Gel (Life Technologies). Proteins were separated in denaturing conditions and transferred to a polyvinylidene difluoride membrane using a wet electroblotting system (Bio-Rad, Hercules, CA) in Tris–glycine buffer containing 10% methanol and 0.02% sodium dodecyl sulfate. Blocking was performed with 5% dry milk powder. The membrane was then incubated with the primary antibodies (ab) diluted in blocking buffer (anti-dysferlin, Novocastra NCL-Hamlet, 1:500, overnight at 4 °C/anti-fast MyHC; Novocastra NCL-MHCf, 1:500, 1 hour at room temperature (RT)/anti-alpha-tubulin; Sigma-Aldrich T6074, 1:2,000, 1 hour at RT/anti-TurboGFP; Evrogen AB513, 1:5,000, overnight at 4 °C) followed by extensive washing. Incubation with the corresponding HRP-conjugated secondary abs was performed at RT for 1 hour. After washing, the membrane was incubated with ECL reagent (GE Healthcare, Milwaukee, WI) for 5 minutes and imaged using a STELLA 3200 system (Raytest, Straubenhardt, Germany). Images were processed using Adobe Photoshop CS5. Any adaptations were applied to the full image with all lanes only.

**Dysferlin immunostaining in cultured myoblasts and myotubes.** For immunofluorescence staining, H2K myoblasts in ibidi wells (80826 ibidi, Planegg, Germany) were fixed for 5 minutes in methanol at –20 °C, washed with phosphate-buffered saline (PBS), and blocked with 1% bovine serum albumin/PBS for 1 hour at RT. Dysferlin was detected using the Romeo ab specific to the N-terminal part of dysferlin (Abcam ab124684, 1:200, Cambridge, UK). After washing, a Cy3-conjugated secondary anti-rabbit ab was added (Jackson ImmunoResearch 711-165-152, 1:500, West Grove, PA). Nuclei were counterstained with 4',6-diamidino-2-phenylindole (1:10,000 in PBS). The wells were washed, sealed, and kept at 4 °C until imaging.

**Mouse experiments.** B6.Cg-Dys<sup>f<sup>rm</sup></sup> Prkdc<sup>scid</sup>/J (Scid/BLA/J) homozygous for the Dys<sup>f<sup>rm</sup></sup> and Prkdc<sup>scid</sup> alleles were purchased from The Jackson Laboratory and bred in our specific pathogen-free animal facility. All animal experiments were performed under the license number G0035/14 (LaGeSo, Berlin, Germany). Focal irradiation of mouse hind limbs was performed as described.<sup>27</sup> For transplantation, cultured H2K myoblasts were washed and resuspended in Dulbecco's Modified Eagle Medium containing 2% fetal calf serum. Eight 12–15-week-old female Scid/BLA/J mice were anesthetized with ketamine-xylazine (9 mg/ml ketamine, 1.2 mg/ml xylazine) in sterile PBS at a dose of 160  $\mu$ l/20 g. The area above the TA was shaved and disinfected and 30  $\mu$ l of cell suspension were injected with a 26-gauge hypodermic needle in the median portion of the TA.



When CTX was applied, 40  $\mu$ l of 10  $\mu$ mol/l CTX/PBS (Latoxan, Valence, France) was injected 1–2 minutes after the cells. At the indicated time points, mice were sacrificed. TA muscles were prepared and cut in two halves following a transversal plane. With the cutting edge atop, each half was separately mounted on cork plates and frozen in liquid nitrogen under cryoprotection. Frozen muscles were stored at  $-80^{\circ}\text{C}$ .

**Immunofluorescence staining of muscle sections.** For dysferlin immunostaining, 6- $\mu$ m transversal cryosections were air-dried for at least 30 minutes at RT and fixed for 5 minutes in acetone at  $-20^{\circ}\text{C}$ . After blocking, they were incubated overnight at  $4^{\circ}\text{C}$  with the Romeo ab (1:100) in 1% bovine serum albumin/PBS. Secondary anti-rabbit Cy3-conjugated ab was applied as above. Nuclei were counterstained with 4',6-diamidino-2-phenylindole (1:5,000). The sections were washed in PBS and ddH<sub>2</sub>O and mounted with Aqua Poly/Mount (Polysciences, Inc, Warrington, PA). For Pax7/laminin immunostaining, 6- $\mu$ m cryosections were fixed in 4% paraformaldehyde, washed, and blocked with 5% bovine serum albumin, 3% donkey serum. After overnight incubation at  $4^{\circ}\text{C}$  with a monoclonal mouse-anti-Pax7 ab (DSHB, Iowa City, IA, supernatant diluted 1:1 in sterile glycerol, working dilution 1:10) and rabbit polyclonal anti-laminin ab (Sigma-Aldrich L-9393, 1:200), sections were washed and incubated with secondary abs against mouse IgG (AlexaFluor 555, life technologies, 1:500) and rabbit IgG (AlexaFluor 647, life technologies, 1:500). Counterstain of nuclei, washing and mounting was performed as above. For Pax7/dysferlin immunostaining, 6- $\mu$ m cryosections were fixed with 4% paraformaldehyde and blocked with 5% bovine serum albumin + 3% donkey serum. The sections were incubated overnight at  $4^{\circ}\text{C}$  with mouse-anti-Pax7 ab (DSHB, stock as above, working dilution 1:5) and Romeo ab (1:50). Incubation with secondary antibodies against mouse and rabbit IgG as well as nuclei counterstaining and mounting were performed as above. H&E, Gomori Trichrome, and NADH-dehydrogenase stainings were performed according to standard protocols.

**Image acquisition and processing.** All image-containing figures were built in Adobe Illustrator CS5 and image graphics were added in Adobe Illustrator CS5. Images from immunofluorescence stainings on cultured cells and mouse muscle cryosections were acquired with a Zeiss LSM 700 confocal microscope and processed with Zen 2012 (Zeiss, Jena, Germany). Dysferlin-positive fibers were counted with the cell counter plugin of ImageJ on confocal microscopy images of cryosections immunostained with the Romeo ab. Images from histological stainings on mouse muscle cryosections were acquired with a Leica DM LB2 microscope (Leica Microsystems, Wetzlar, Germany) and processed with Adobe Photoshop CS5. All modifications were always applied to the full image.

## Supplementary material

**Figure S1.** SB transposition in H2K A/J myoblasts.

**Acknowledgments** The work was supported by the German Research Society (DFG) through GK1631 “MyoGrad” and KFO192 (Sp1152/8-1). There is no conflict of interest. H.E. performed all experiments. V.S. helped with the animal experi-

ments. S.S. designed the study, discussed data, and wrote the manuscript. A.M. performed immunofluorescence, designed experiments, and discussed data. Z.I. supervised and discussed the experiments using the Sleeping Beauty based vector. Z.I. was supported by ERC-2011-AdG 294742. H.E. was supported by GK1631 and by the Association française contre les myopathies (AFM-Téléthon). The authors thank Terence Partridge for providing H2K and H2K A/J cells and Adrienne Rothe and Kornelia Gräning for excellent technical assistance.

- Liu, J, Aoki, M, Illa, I, Wu, C, Fardeau, M, Angelini, C et al. (1998). Dysferlin, a novel skeletal muscle gene, is mutated in Miyoshi myopathy and limb girdle muscular dystrophy. *Nat Genet* **20**: 31–36.
- Bashir, R, Britton, S, Strachan, T, Keers, S, Vafiadaki, E, Lako, M et al. (1998). A gene related to *Caenorhabditis elegans* spermatogenesis factor fer-1 is mutated in limb-girdle muscular dystrophy type 2B. *Nat Genet* **20**: 37–42.
- Illa, I, Serrano-Munuera, C, Gallardo, E, Lasa, A, Rojas-García, R, Palmer, J et al. (2001). Distal anterior compartment myopathy: a dysferlin mutation causing a new muscular dystrophy phenotype. *Ann Neurol* **49**: 130–134.
- Aoki, M, Liu, J, Richard, I, Bashir, R, Britton, S, Keers, SM et al. (2001). Genomic organization of the dysferlin gene and novel mutations in Miyoshi myopathy. *Neurology* **57**: 271–278.
- Lek, A, Evesson, FJ, Sutton, RB, North, KN and Cooper, ST (2012). Ferlins: regulators of vesicle fusion for auditory neurotransmission, receptor trafficking and membrane repair. *Traffic* **13**: 185–194.
- Anderson, LV, Davison, K, Moss, JA, Young, C, Cullen, MJ, Walsh, J et al. (1999). Dysferlin is a plasma membrane protein and is expressed early in human development. *Hum Mol Genet* **8**: 855–861.
- De Luna, N, Gallardo, E and Illa, I (2004). *In vivo* and *in vitro* dysferlin expression in human muscle satellite cells. *J Neuropathol Exp Neurol* **63**: 1104–1113.
- Ampong, BN, Imamura, M, Matsumiya, T, Yoshida, M and Takeda, S (2005). Intracellular localization of dysferlin and its association with the dihydropyridine receptor. *Acta Myol* **24**: 134–144.
- Kerr, JP, Ziman, AP, Mueller, AL, Muriel, JM, Kleinhans-Welte, E, Gumerson, JD et al. (2013). Dysferlin stabilizes stress-induced Ca<sup>2+</sup> signaling in the transverse tubule membrane. *Proc Natl Acad Sci USA* **110**: 20831–20836.
- Bansal, D, Miyake, K, Vogel, SS, Groh, S, Chen, CC, Williamson, R et al. (2003). Defective membrane repair in dysferlin-deficient muscular dystrophy. *Nature* **423**: 168–172.
- Wenzel, K, Zabojszcza, J, Carl, M, Taubert, S, Lass, A, Harris, CL et al. (2005). Increased susceptibility to complement attack due to down-regulation of decay-accelerating factor/CD55 in dysferlin-deficient muscular dystrophy. *J Immunol* **175**: 6219–6225.
- Han, R, Frett, EM, Levy, JR, Rader, EP, Lueck, JD, Bansal, D et al. (2010). Genetic ablation of complement C3 attenuates muscle pathology in dysferlin-deficient mice. *J Clin Invest* **120**: 4366–4374.
- Swierczek, M, Izsvák, Z and Ivics, Z (2012). The Sleeping Beauty transposon system for clinical applications. *Expert Opin Biol Ther* **12**: 139–153.
- Izsvák, Z, Ivics, Z and Plasterk, RH (2000). Sleeping Beauty, a wide host-range transposon vector for genetic transformation in vertebrates. *J Mol Biol* **302**: 93–102.
- Mátés, L, Chuah, MK, Belay, E, Jerchow, B, Manoj, N, Acosta-Sanchez, A et al. (2009). Molecular evolution of a novel hyperactive Sleeping Beauty transposase enables robust stable gene transfer in vertebrates. *Nat Genet* **41**: 753–761.
- Rostovskaya, M, Fu, J, Obst, M, Baer, I, Weidlich, S, Wang, H et al. (2012). Transposon-mediated BAC transgenesis in human ES cells. *Nucleic Acids Res* **40**: e150.
- Kebrl, P, Huls, H, Jena, B, Munsell, M, Jackson, R, Lee, DA et al. (2012). Infusing CD19-directed T cells to augment disease control in patients undergoing autologous hematopoietic stem-cell transplantation for advanced B-lymphoid malignancies. *Hum Gene Ther* **23**: 444–450.
- Cohen, TV, Cohen, JE and Partridge, TA (2012). Myogenesis in dysferlin-deficient myoblasts is inhibited by an intrinsic inflammatory response. *Neuromuscul Disord* **22**: 648–658.
- Morgan, JE, Beauchamp, JR, Pagel, CN, Peckham, M, Ataliotis, P, Jat, PS et al. (1994). Myogenic cell lines derived from transgenic mice carrying a thermolabile T antigen: a model system for the derivation of tissue-specific and mutation-specific cell lines. *Dev Biol* **162**: 486–498.
- Ho, M, Post, CM, Donahue, LR, Lidov, HG, Bronson, RT, Goolsby, H et al. (2004). Disruption of muscle membrane and phenotype divergence in two novel mouse models of dysferlin deficiency. *Hum Mol Genet* **13**: 1999–2010.
- Jat, PS, Noble, MD, Ataliotis, P, Tanaka, Y, Yannoutsos, N, Larsen, L et al. (1991). Direct derivation of conditionally immortal cell lines from an H-2Kb-tsA58 transgenic mouse. *Proc Natl Acad Sci USA* **88**: 5096–5100.
- Farini, A, Sitzia, C, Navarro, C, D'Antona, G, Belicchi, M, Parolini, D et al. (2012). Absence of T and B lymphocytes modulates dystrophic features in dysferlin deficient animal model. *Exp Cell Res* **318**: 1160–1174.



23. Li, X, Eastman, EM, Schwartz, RJ and Draghia-Akli, R (1999). Synthetic muscle promoters: activities exceeding naturally occurring regulatory sequences. *Nat Biotechnol* **17**: 241–245.
24. Foster, H, Sharp, PS, Athanasopoulos, T, Trollet, C, Graham, IR, Foster, K *et al.* (2008). Codon and mRNA sequence optimization of microdystrophin transgenes improves expression and physiological outcome in dystrophic mdx mice following AAV2/8 gene transfer. *Mol Ther* **16**: 1825–1832.
25. Koo, T, Malerba, A, Athanasopoulos, T, Trollet, C, Boldrin, L, Ferry, A *et al.* (2011). Delivery of AAV2/9-microdystrophin genes incorporating helix 1 of the coiled-coil motif in the C-terminal domain of dystrophin improves muscle pathology and restores the level of  $\alpha$ 1-syntrophin and  $\alpha$ -dystrobrevin in skeletal muscles of mdx mice. *Hum Gene Ther* **22**: 1379–1388.
26. Boldrin, L, Neal, A, Zammit, PS, Muntoni, F and Morgan, JE (2012). Donor satellite cell engraftment is significantly augmented when the host niche is preserved and endogenous satellite cells are incapacitated. *Stem Cells* **30**: 1971–1984.
27. Marg, A, Escobar, H, Gloy, S, Kufeld, M, Zacher, J, Spuler, A *et al.* (2014). Human satellite cells have regenerative capacity and are genetically manipulable. *J Clin Invest* **124**: 4257–4265.
28. Briggs, D and Morgan, JE (2013). Recent progress in satellite cell/myoblast engraftment – relevance for therapy. *FEBS J* **280**: 4281–4293.
29. Duchen, LW, Excell, BJ, Patel, R and Smith, B (1974). Changes in motor end-plates resulting from muscle fibre necrosis and regeneration. A light and electron microscopic study of the effects of the depolarizing fraction (cardiotoxin) of *Dendroaspis jamesoni* venom. *J Neurol Sci* **21**: 391–417.
30. Seale, P, Sabourin, LA, Girgis-Gabardo, A, Mansouri, A, Gruss, P and Rudnicki, MA (2000). Pax7 is required for the specification of myogenic satellite cells. *Cell* **102**: 777–786.
31. MAURO, A (1961). Satellite cell of skeletal muscle fibers. *J Biophys Biochem Cytol* **9**: 493–495.
32. Leriche-Guérin, K, Anderson, LV, Wroegemann, K, Roy, B, Goulet, M and Tremblay, JP (2002). Dysferlin expression after normal myoblast transplantation in SCID and in SJL mice. *Neuromuscul Disord* **12**: 167–173.
33. Grose, WE, Clark, KR, Griffin, D, Malik, V, Shontz, KM, Montgomery, CL *et al.* (2012). Homologous recombination mediates functional recovery of dysferlin deficiency following AAV5 gene transfer. *PLoS One* **7**: e39233.
34. Sondergaard, PC, Griffin, DA, Pozsgai, ER, Johnson, RW, Grose, WE, Heller, KN *et al.* (2015). AAV-Dysferlin overlap vectors restore function in dysferlinopathy animal models. *Ann Clin Transl Neurol* **2**: 256–270.
35. Lostal, W, Bartoli, M, Bourg, N, Roudaut, C, Bentaib, A, Miyake, K *et al.* (2010). Efficient recovery of dysferlin deficiency by dual adeno-associated vector-mediated gene transfer. *Hum Mol Genet* **19**: 1897–1907.
36. Wang, D, Zhong, L, Nahid, MA and Gao, G (2014). The potential of adeno-associated viral vectors for gene delivery to muscle tissue. *Expert Opin Drug Deliv* **11**: 345–364.
37. Meregalli, M, Navarro, C, Sitzia, C, Farini, A, Montani, E, Wein, N *et al.* (2013). Full-length dysferlin expression driven by engineered human dystrophic blood derived CD133<sup>+</sup> stem cells. *FEBS J* **280**: 6045–6060.
38. Sinnreich, M, Therrien, C and Karpati, G (2006). Lariat branch point mutation in the dysferlin gene with mild limb-girdle muscular dystrophy. *Neurology* **66**: 1114–1116.
39. Wein, N, Avril, A, Bartoli, M, Beley, C, Chaouch, S, Laforêt, P *et al.* (2010). Efficient bypass of mutations in dysferlin deficient patient cells by antisense-induced exon skipping. *Hum Mutat* **31**: 136–142.
40. Philippi, S, Lorain, S, Beley, C, Peccate, C, Précigout, G, Spuler, S *et al.* (2015). Dysferlin rescue by spliceosome-mediated pre-mRNA trans-splicing targeting introns harbouring weakly defined 3' splice sites. *Hum Mol Genet* **24**: 4049–4060.
41. Dominov, JA, Uyan, O, Sapp, PC, McKenna-Yasek, D, Nallamilli, BR, Hegde, M *et al.* (2014). A novel dysferlin mutant pseudoexon bypassed with antisense oligonucleotides. *Ann Clin Transl Neurol* **1**: 703–720.
42. Morgan, JE, Gross, JG, Pagel, CN, Beauchamp, JR, Fassati, A, Thrasher, AJ *et al.* (2002). Myogenic cell proliferation and generation of a reversible tumorigenic phenotype are triggered by preirradiation of the recipient site. *J Cell Biol* **157**: 693–702.
43. Meng, J, Bencze, M, Asifhani, R, Muntoni, F and Morgan, JE (2015). The effect of the muscle environment on the regenerative capacity of human skeletal muscle stem cells. *Skelet Muscle* **5**: 11.
44. Sambasivan, R, Yao, R, Kissenpfennig, A, Van Wittenbergh, L, Paldi, A, Gayraud-Morel, B *et al.* (2011). Pax7-expressing satellite cells are indispensable for adult skeletal muscle regeneration. *Development* **138**: 3647–3656.
45. Lepper, C, Partridge, TA and Fan, CM (2011). An absolute requirement for Pax7-positive satellite cells in acute injury-induced skeletal muscle regeneration. *Development* **138**: 3639–3646.
46. Díaz-Manera, J, Touvier, T, Dellavalle, A, Tonlorenzi, R, Tedesco, FS, Messina, G *et al.* (2010). Partial dysferlin reconstitution by adult murine mesoangioblasts is sufficient for full functional recovery in a murine model of dysferlinopathy. *Cell Death Dis* **1**: e61.
47. Skuk, D, Paradis, M, Goulet, M, Chappelaine, P, Rothstein, DM and Tremblay, JP (2010). Intramuscular transplantation of human postnatal myoblasts generates functional donor-derived satellite cells. *Mol Ther* **18**: 1689–1697.
48. Wenzel, K, Carl, M, Perrot, A, Zabojszcza, J, Assadi, M, Ebeling, M *et al.* (2006). Novel sequence variants in dysferlin-deficient muscular dystrophy leading to mRNA decay and possible C2-domain misfolding. *Hum Mutat* **27**: 599–600.
49. Glover, LE, Newton, K, Krishnan, G, Bronson, R, Boyle, A, Krivickas, LS *et al.* (2010). Dysferlin overexpression in skeletal muscle produces a progressive myopathy. *Ann Neurol* **67**: 384–393.
50. Huang, X, Guo, H, Tammana, S, Jung, YC, Mellgren, E, Bassi, P *et al.* (2010). Gene transfer efficiency and genome-wide integration profiling of Sleeping Beauty, Tol2, and piggyBac transposons in human primary T cells. *Mol Ther* **18**: 1803–1813.
51. Moldt, B, Miskey, C, Staunstrup, NH, Gogol-Döring, A, Bak, RO, Sharma, N *et al.* (2011). Comparative genomic integration profiling of Sleeping Beauty transposons mobilized with high efficacy from integrase-defective lentiviral vectors in primary human cells. *Mol Ther* **19**: 1499–1510.
52. Grabundzija, I, Wang, J, Sebe, A, Erdei, Z, Kajdi, R, Devaraj, A *et al.* (2013). Sleeping Beauty transposon-based system for cellular reprogramming and targeted gene insertion in induced pluripotent stem cells. *Nucleic Acids Res* **41**: 1829–1847.
53. Schoewel, V, Marg, A, Kunz, S, Overkamp, T, Carrazedo, RS, Zacharias, U *et al.* (2012). Dysferlin-peptides reallocate mutated dysferlin thereby restoring function. *PLoS One* **7**: e49603.



This work is licensed under a Creative Commons Attribution-NonCommercial-NoDerivs 4.0 International License. The images or other third party material in this article are included in the article's Creative Commons license, unless indicated otherwise in the credit line; if the material is not included under the Creative Commons license, users will need to obtain permission from the license holder to reproduce the material. To view a copy of this license, visit <http://creativecommons.org/licenses/by-nc-nd/4.0/>

Supplementary Information accompanies this paper on the Molecular Therapy–Nucleic Acids website (<http://www.nature.com/mtna>)